

HETEROCYCLES, Vol. 81, No. 3, 2010, pp. 659 - 674. © The Japan Institute of Heterocyclic Chemistry
Received, 18th December, 2009, Accepted, 29th January, 2010, Published online, 1st February, 2010
DOI: 10.3987/COM-09-11889

EFFECT OF NITRO-SUBSTITUTION ON THE PHOTOCHEMISTRY OF 3-PIPERIDINO-1,2-BENZISOTHIAZOLE DERIVATIVES: A MECHANISTIC INVESTIGATION

Hiroharu Tanikawa, Kazuhiro Ishii, Shun Kubota, Takashi Sasanuma, Shiki Yagai, Akihide Kitamura, and Takashi Karatsu*

Department of Applied Chemistry and Biotechnology, Graduate School of Engineering, Chiba University, 1-33 Yayoi-cho, Inage-ku, Chiba, 263-8522, Japan, e-mail address: karatsu@faculty.chiba-u.jp

Abstract – Photochemical isomerization of 3-piperidino-1,2-benzisothiazole (BIT)–benzothiazole (BT) was investigated. In particular, the effect of nitro-substitution on the benzene ring was selectively examined for the parent, 5-nitro-, and 7-nitro-derivatives. 3-Piperidino-BIT and nitro-3-piperidino-BIT isomerized irreversibly to the corresponding 2-piperidino-BT, and this reaction mechanism was investigated using density-functional theory (DFT) and time-dependent (TD)-DFT calculations. These calculations showed that this isomerization goes through an azirine intermediate. In addition, excitation wavelength effect demonstrates that isomerization occurs from the upper excited state of nitro-derivatives. The HOMO-LUMO transition has charge-transfer and photoinactive characters.

INTRODUCTION

Benzisothiazoles (BIT) and benzothiazoles (BT) skeletons are often found in pharmaceutically and agriculturally active chemicals, and possess key functions. For example, ziprasidone (as Zeldox from Pfizer), which has a BIT skeleton, is approved by US-FDA,¹ and is now being used as an antipsychotic drug. Riluzole (as Rilutek from Sanofi-Aventis), which has a BT skeleton, is an authorized medicine for amyotrophic lateral sclerosis (ALS).² The BT structured KIF-230 (as Benthiavalicarb from Kumiai Chemicals) is also used as an antifungal agricultural chemical.³ If BIT–BT photoisomerization is found to occur, this reaction could become a valuable tool in the synthesis of BIT and BT derivatives with similar substituents, while they are currently synthesized by completely separate methods.

Five-membered aromatic compounds containing of two heteroatoms, such as isothiazoles–thiazoles,⁴⁻⁷ or isooxazoles–oxazoles,⁴⁻⁷ have been studied in depth and are known to undergo reversible photoisomerization. However, the photochemical behavior of their condensed ring analogues has not been widely studied. This study focuses on the increasingly important photochemical BIT–BT isomerization reaction, while, partial photoisomerization has been observed during photostability testing of ziprasidone,⁸ better understanding and control of this reaction should be very important in the design of new drugs.

Our preliminary paper⁹ deals with 3-piperidino-5-nitrobenzisothiazole derivatives because of their highly selective photochemical reactions (Fig.1, **1a**). The nitro-group does not often feature in biological processes; however, compounds involving a nitro group are easy to detect, and allow conversion to various functional groups, such as amines, imines, amides, and halides. In this paper, to clarify the function of the nitro-groups in the photochemical reactivity of **1a**, photoreaction of **1b** ($R_1=H$, $R_2=NO_2$) and **1c** ($R_1=H$, $R_2=H$) for the photochemical isomerization of 3-piperidinobenzisothiazole to piperidinobenzothiazole were studied using density functional theory (DFT) and time-dependent (TD)-DFT.

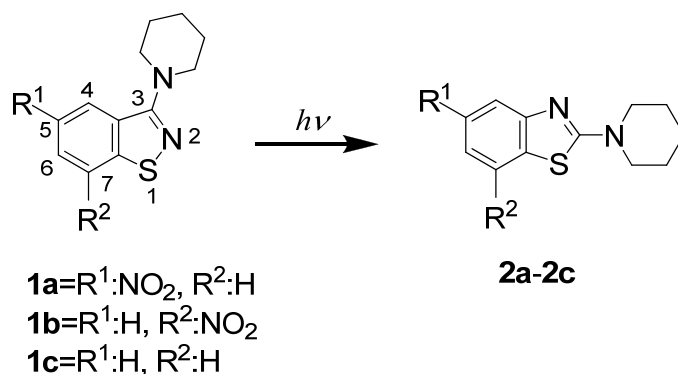


Figure 1. Photochemical isomerization of 3-piperidino-1,2-benzisothiazole derivatives (**1a-c**) to benzothiazole derivatives (**2a-c**)

RESULTS AND DISCUSSION

When a solution of **1b** in acetonitrile (3 mL, 3.9×10^{-4} M) purged by argon was exposed to a 400 W Xe-arc lamp through a quartz cuvette using UV30 glass filter (> 300 nm), no photochemical reactions were observed. However, using a low-pressure mercury lamp (254 nm) for 24 h, UV–Vis absorption analyses showed clear isosbestic points at 255 and 377 nm. 254 nm-Photolysis of **1b** gave **2b** in 46% yield (Figure 2). Reverse phase HPLC analysis of reaction mixture showed **2b** as the only separable product. Spectral identification of the BIT and BT structures were difficult, however, the 4, 6, and 7 positions proton signals were slight shifted to the higher magnetic field after the isomerization (**1a**→**2a**, $\delta = 8.79 \rightarrow 8.31$ (H4), $8.30 \rightarrow 7.91$ (H6), $7.89 \rightarrow 7.65$ (H7), see details in experimental section) indicating a

decreasing electron density in the benzene ring of BT compared to that of BIT (i.e., due to BIT→BT isomerization). The spectral data of **2b** were identical to those of the separately synthesized substance, 7-nitro-2-piperidino-1,3-benzothiazole. Noticeably, irradiation of **2b** did not produce **1b**. Therefore, the BIT→BT isomerization is one-way, and not reversible.

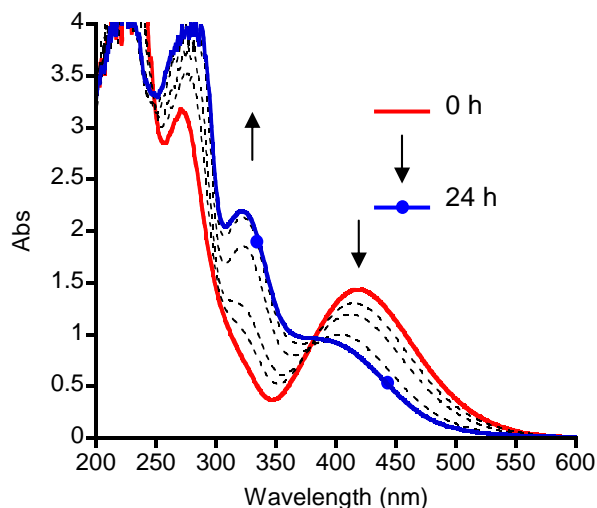


Figure 2. Absorption spectral change of **1b** by irradiation of 254 nm light in MeCN (3.9×10^{-4} M)

Photoreactions of **1b** were also examined in methanol and *n*-hexane purged by argon (1.5×10^{-4} M), as shown in Figure 3. The isomerization cleanly produced **2b** as the sole photo-product. The reaction was accelerated two-fold in methanol. On the other hand, photoirradiation of **1b** produced in several inseparable products in *n*-hexane. This reaction was also examined under oxygen-saturated acetonitrile. The complete spectral change of **1b** to **2b** under oxygen was identical to that under argon. Therefore, we conclude that this reaction was not quenched by oxygen and may occur via a electronically singlet-excited state (S_1) with a short lifetime.

To supplement our findings, we conducted two control experiments. No isomerization was observed when **1a** was irradiated with light of wavelength greater than 300 nm (irradiation was performed using a 500W Xe arc lamp with UV30 HOYA glass filter). The reaction of **1a** was also examined in the presence of trifluoroacetic acid (TFA) for protonating the amino group. However, TFA had no effect on the photochemical isomerization reaction. From the results of solvent effect, we expected that the isomerization proceeds through polar intermediate which has charge transfer nature from piperidino nitrogen to the nitrobenzothiazole moiety, however, no effect was observed by protonation of the piperidino nitrogen to reduce electron donating character.

Figure 4 shows the absorption spectral change of **1c** in acetonitrile after 10 h of irradiation. The initial spectrum of **1c** changed cleanly to the product spectrum, with isosbestic points at 220, 252, 306 nm (Figure 4a). The spectrum of the product is absolutely consistent with the spectrum of **2c** synthesized

separately (Figure 4b).

Irradiation of **1a**, **1b**, and **1c** induced BIT \rightleftharpoons BT isomerization. However, irradiation of **2a**, **2b**, and **2c** induced no BT \rightleftharpoons BIT isomerization. Therefore, this isomerization proceeded as BIT \rightleftharpoons BT one-way isomerization. The absorption maxima of BT derivatives usually locate at shorter wavelengths than the corresponding BIT derivatives, and therefore, lowest excitation energies of **2a** and **2c** are expected to be higher than that of the primary azirine-type intermediate (spiroazacyclopropene) **IM1** except in the case of **2b**.

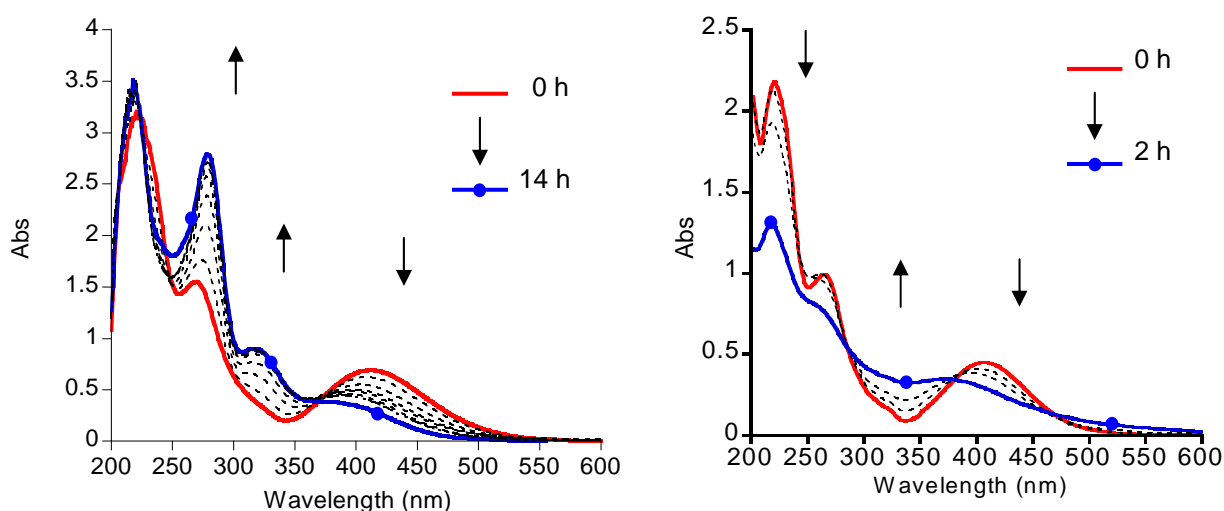


Figure 3. Absorption spectra change of **1b** by irradiation of 254 nm light in MeOH (left) and in *n*-hexane (right), 1.5×10^{-4} M

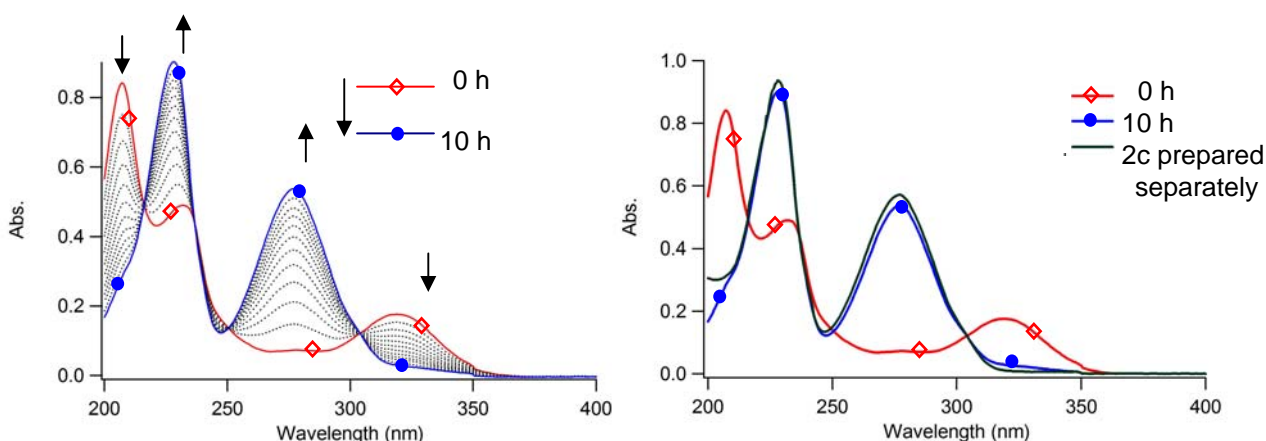


Figure 4. Absorption spectra change of **1c** by irradiation of 254 nm light in MeCN

Figure 5 shows a plausible isomerization mechanism proposed in our preliminary paper, and Figure 6 shows an energy diagram of the reactants, products, and possible reaction intermediates appearing in Figure 5. This reaction mechanism is proposed on the basis of the reported isothiazole–thiazole

photoisomerization via an azirine (**IM1**) after the breakage of the S–N bond.^{5a} The reaction may generate Dewar benzisothiazole (**IM2**), isomerizes to azirine (**IM1**), and finally gives **2**. This reaction may proceed stepwise from S_1 of **1**→**IM2**→**IM1**, or from S_1 of **1** to **IM3**→**IM2**→**IM1**. Alternatively, this reaction may proceed directly from S_1 of **1**→**IM1** by skipping some steps in the formation of **IM1**. In addition, the step involving N–S bond dissociation is unclear, since there are no experimental data. Recently, similar reaction mechanisms have been reported in the study of Sipos *et al.*^{5c} There is a possibility that this reaction proceeds through electrocyclic ring closure, and sigmatropic shift of sulfur atom around the four sides of azetidine ring (**IM2**, **IM3**, **IM4**).^{5b}

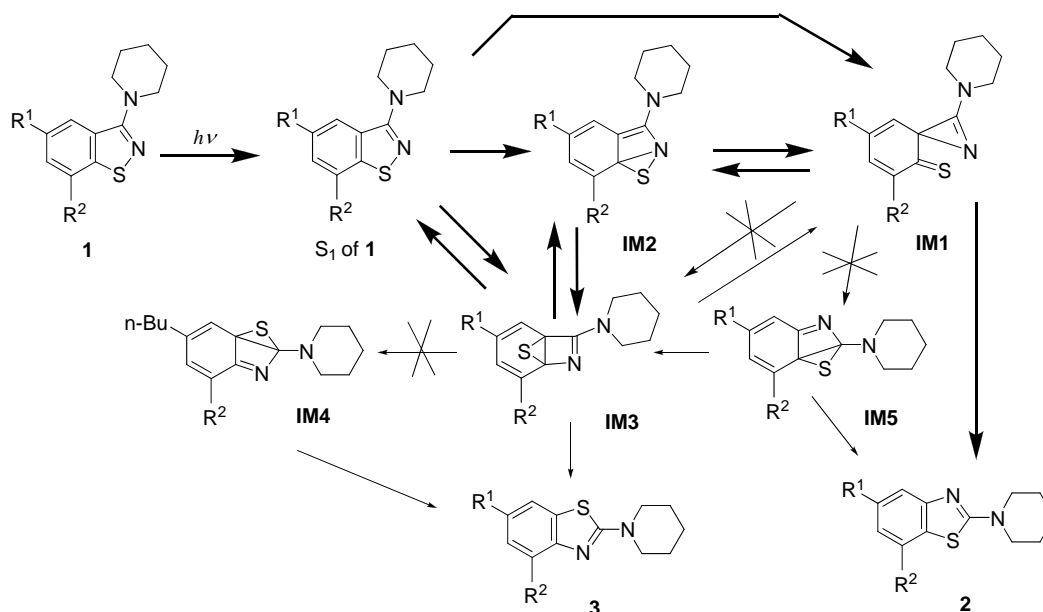


Figure 5. Plausible mechanism of the photochemical isomerization of **1a**, **1b**, or **1c**

Figure 6 indicates energetic aspect of this mechanism. The reaction initiates from a S_1 of **1a**, **1b**, and **1c**, generated by UV irradiation. S_1 state energies of **1a**, **1b**, and **1c** calculated from the longest absorption band maxima of UV absorption spectra are 68.1, 71.9, and 92.0 kcal mol⁻¹ higher than the values calculated for the corresponding ground-state reactants, respectively. The S_1 of **1a**, **1b**, or **1c** forms azirine (**IM1**, 52.1, 60.3 and 39.8 kcal mol⁻¹ for **a**, **b**, and **c**, respectively), or a Dewar-type isomer (**IM2**, 51.4, 61.6 and 41.3 kcal mol⁻¹ for **a**, **b**, and **c**, respectively). Other isomeric intermediates (**IM3-IM5**) may not be formed because they have higher energies than those of **IM1** and **IM2**, and also S_1 energies of **1a** and **1b**. Relative energy differences ΔE of the corresponding reactant and product were 12.5, 12.1, and 23.1 kcal mol⁻¹, for **1a-2a**, **1b-2b**, and **1c-2c**, respectively, by DFT calculation (Figure 6) indicating these reactions exothermic.

The effect of the nitro-group on the BIT→BT photoisomerization was considered. The yields of isomerization of 3-piperadino-BIT to BT achieved are summarized in Table 1. BIT→BT

photoisomerization yield of **1c** was the highest (91%), and **1b** was the lowest (46%). **1c** has no nitro-group as a substituent, and no absorption at the wavelength longer than 350 nm (Figure 7c). Therefore, the S_1 state of **1c** is 92 kcal mol⁻¹ above the ground state. In **1b**, an introduction of a nitro-group at 7-position of BIT brought a significant red-shift in the absorption spectra, and the tail reached to 550 nm. The longest absorption maximum was 407 nm, and this corresponds to S_1 of **1b**, located 71.9 kcal mol⁻¹ higher than the ground state.

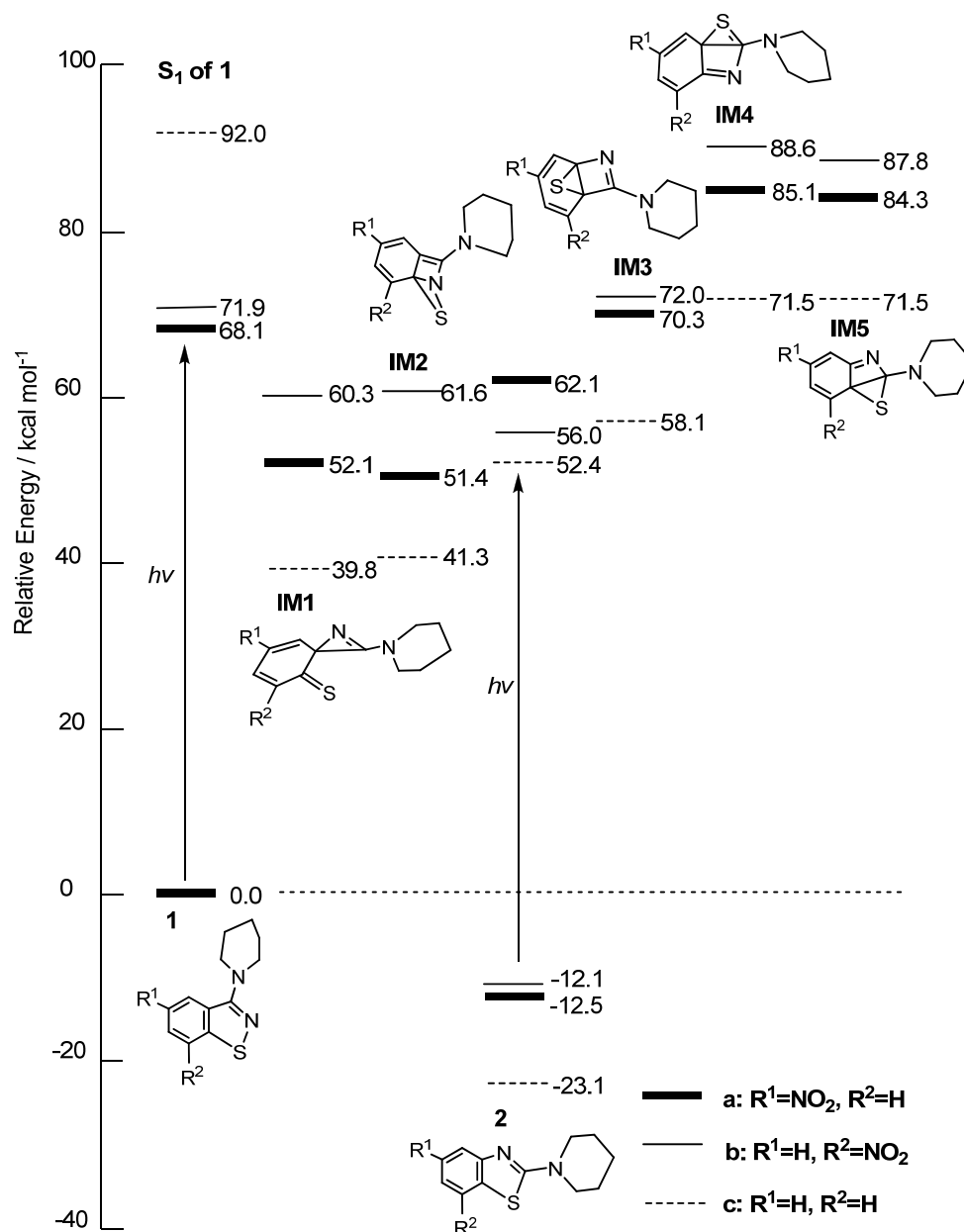


Figure 6. Relative energies calculated by DFT method for the reactant (**1**), product (**2**), and intermediates (**IM**) considered in the photoisomerization

1c has no absorption longer than 350 nm. Calculated oscillator strength at 318 nm was 0.074, and this transition is ascribed to HOMO→LUMO transition. In energy diagram of **1c**, S_1 locates much higher in

energy than other intermediates. However, once **1c** generates azirine intermediate (**IM1**), it is difficult to isomerize to **IM3-5** by the reason of energetic requirement.

Compound **3** is another possible photoproduct. We have reported that an irradiation of 3-*n*-butylamino-5-nitrobenzothiazole (**1d**) is the only case obtaining **3**-type product (3-amino-6-nitrobenzothiazole: **3e**) through the isomerization to **3d** and dealkylation giving **3e** (Figure 7).⁹ This product **3d** (N and S atom positions were inverted by the typical expecting product **2d**) was not isolable, and a control experiment showed **1e** did not give **3e**. This reaction is useful to introduce a nitro-group to 6-position in the benzothiazole skeleton. However, we could not observe this type of photoproducts from the photoreaction of **1a** and **1b**. Formation of **3d** requires sulfur-atom migration along the isothiazole ring (the second row, **IM4**, **IM3**, and **IM5** in Figure 5) which is an energetically unfavorable (endothermic) process (Figure 6). In the case of **1c**, it is hard to exclude this reaction, because **3d** corresponds to **2c** in case of no nitro-substituent.

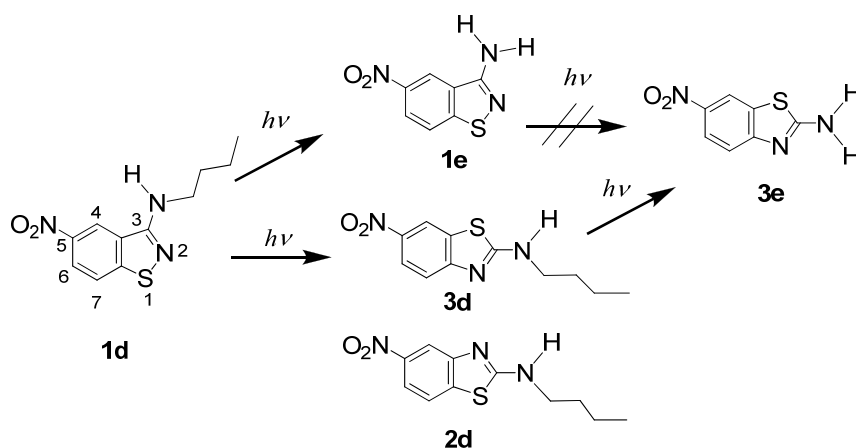


Figure 7. Photochemical reaction of **1d** produced **3e** through the photoreaction of **3d**

Table 1 summarizes the substituents, isomerization yield, and the energy difference between the singlet-excited state and the reaction intermediates in the BIT→BT isomerization. BIT→BT isomerization yields increase with the increase in exothermicity from the singlet-excited state of the reactant to the azirine **IM1**. Higher exothermicity (S_1 of **1a** and **1c** to corresponding **IM1**) (52.2 and 16.0 kcal mol⁻¹) leads to higher yields (91 and 87%, respectively), and lower exothermicity (11.6 kcal mol⁻¹) leads to a lower yield (46%). This may be explained by the Hammond's hypothesis that higher exothermic reaction requires smaller activation energy.

The electronic transitions of the ground state to low-lying eight singlet-excited states obtained by TD-DFT method are shown in Table 2, and their energies and oscillator strengths are superimposed in the absorption spectra (Figure 8). Figure 9 shows molecular orbitals involving in the transition. The longest wavelength transition is predominantly ascribed to HOMO–LUMO transition (weight of HOMO–LUMO

is nearly 70%). The transition energies appeared lower in energy than the observed absorption bands for **1a** and **1b**, but appeared in the same position for **1c**. Transition in the higher energies of **1a** and **1b** are mostly from occupied molecular orbitals (MO) lower than HOMO to LUMO. Molecular orbital analysis showed that HOMO–LUMO transition of **1a–b** has a charge-transfer (CT) character. HOMO mainly localized at piperidino–nitrogen atom (N1') and isothiazole moiety (S, N2, C3, and C9), and LUMO localized at nitro moiety as seen in HOMO–LUMO in left and center column of Figure 9.

Table 1. Reaction yield and exothermicity from singlet excited state of reactant to intermediates

Reaction	R ¹	R ²	2 yield	$\Delta E_{S1}-\Delta E_{IM}$ (kcal mol ⁻¹)				
				IM1	IM2	IM3	IM4	IM5
1a → 2a	NO ₂	H	87%	16.0	16.7	6.0	-17.0	-16.2
1b → 2b	H	NO ₂	46%	11.6	10.3	0.1	-16.7	-15.9
1c → 2c	H	H	91%	52.2	50.7	39.6	20.5	20.5

Table 2. Electronic transition of ground state to singlet-excited state of **1a**, **1b**, and **1c** calculated by TD-DFT method.

Compounds	Main Transition	(MO #)	Weight of config.	λ_{max}/nm	<i>f</i> : oscillator strength	
1a : 5NO ₂	Entry 1	HOMO →LUMO	(69→70)	0.68	437	0.060
	2	HOMO-3 →LUMO	(66→70)	0.60	333	0.000
	3	HOMO →LUMO+1	(69→71)	0.64	328	0.041
	4	HOMO-1 →LUMO	(68→70)	0.64	306	0.036
	5	HOMO-6 →LUMO	(63→70)	0.61	290	0.001
	6	HOMO-2 →LUMO	(67→70)	0.59	285	0.175
	7	HOMO →LUMO+2	(69→72)	0.51	269	0.009
	8	HOMO-4 →LUMO	(65→70)	0.55	252	0.000
1b : 7NO ₂	Entry 1	HOMO →LUMO	(69→70)	0.68	476	0.064
	2	HOMO-3 →LUMO	(66→70)	0.48	334	0.003
	3	HOMO-1 →LUMO	(68→70)	0.58	321	0.007
	4	HOMO-2 →LUMO	(67→70)	0.51	305	0.004
	5	HOMO-6 →LUMO	(63→70)	0.55	292	0.064
	6	HOMO →LUMO+1	(69→71)	0.52	289	0.064
	7	HOMO-4 →LUMO	(65→70)	0.45	272	0.001
	8	HOMO →LUMO+2	(69→72)	0.69	264	0.023
1c :	Entry 1	HOMO →LUMO	(58→59)	0.66	318	0.074
	2	HOMO →LUMO+1	(58→60)	0.55	275	0.023
	3	HOMO →LUMO+3	(58→62)	0.37	269	0.024
	4	HOMO-1 →LUMO	(57→59)	0.42	255	0.008

5	HOMO-1 → LUMO	(57 → 59)	0.48	252	0.003
6	HOMO → LUMO+4	(58 → 63)	0.60	237	0.013
7	HOMO → LUMO+5	(58 → 64)	0.53	234	0.023
8	HOMO → LUMO+5	(58 → 64)	0.44	233	0.124

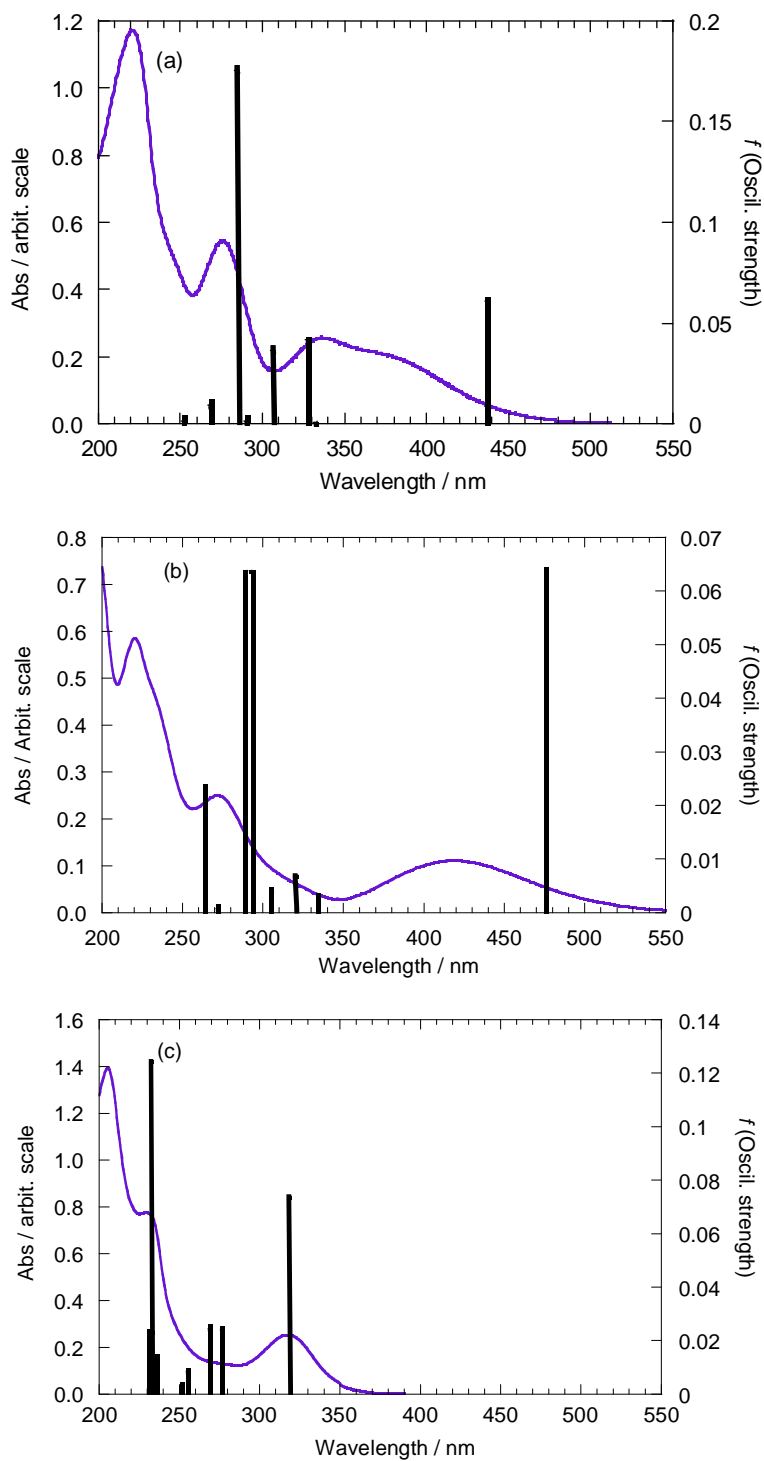


Figure 8. Absorption spectra of (a) **1a**, (b) **1b** and (c) **1c** in acetonitrile, and their oscillator strengths calculated by TD-DFT method

On the other hand, transitions of **1c** are more complicated. Most transitions have a character from HOMO to LUMO or MOs higher than LUMO (i.e. LUMO + n , $n = 1, 3, \text{ or } 5$). The LUMO of **1c** has the same nature as LUMO + 1 of **1a** and **1b** (Figure 8). These LUMO + 1 and LUMO of **1c** orbitals have an anti-bonding π -orbital character of the S–N bond of the isothiazole ring. Therefore, the isomerization may proceed through these excitations and the following bond dissociation of S–N. Characteristic transitions having high oscillator strengths are HOMO–(LUMO + 1) transition (those are entry 3 of **1a** [328 nm] and entry 6 of **1b** [289 nm]), and the HOMO–LUMO transition of **1c**. These transitions have an intramolecular charge transfer nature from piperidino- to nitro-groups as mentioned above. No isomerization was observed by the excitation of the longest absorption band of **1a** and **1b**. These results were consistent with the above results, and the LUMO orbital is the origin of photo-inactiveness by irradiation at longest wavelength absorption band. In photochemistry, upper excited state usually undergoes internal deactivation to the lowest excited state known as Kasha's rule. However, photoisomerization of **1a** and **1b** may occur through higher excited state. The lifetime of this higher excited state is expected to be very short. Therefore photoisomerization was unaffected by oxygen.

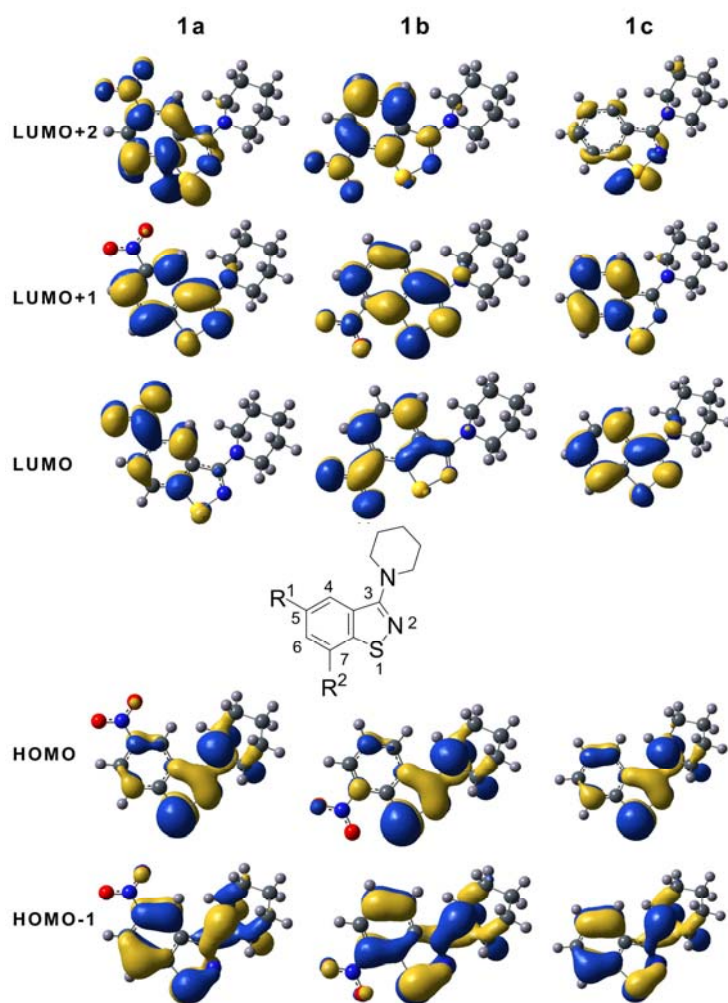


Figure 9. Molecular orbitals of **1a**, **1b**, and **1c** obtained by TD-DFT B3LYP/6-31++G(d) method

In conclusion, we described in this paper the photochemical isomerization mechanisms of the parent, 5-nitro- and 7-nitro-substituted 3-piperidino-1,2-benzisothiazole–benzothiazole derivatives on the basis of experimental and DFT calculated investigations. These isomerizations proceeded from BIT to BT cleanly one-way, and proceeded selectively through the singlet-excited state. In addition, excitation wavelength effect demonstrates that isomerization occurs as a result of excitation to the upper excited state of nitro-derivatives. The HOMO–LUMO transition of nitro-derivatives is inactive due to the charge-transfer nature from piperidino nitrogen and isothiazole ring to the nitrobenzo moiety assigned by MOs. This isomerization initiates from the excited states having dissociative S–N bond character (LUMO of parent, and LUMO+1 of nitro-derivatives), and goes through an azirine intermediate.

EXPERIMENTAL

Instrumentation: ^1H NMR and ^{13}C NMR spectra were recorded on JEOL JNM-LA 400 and Bruker AVANCE 300. Mass spectra (FAB or GC-MS) were recorded on a JEOL JMS-AX500 double focusing mass spectrometer or Shimadzu PARVUM 2 GC-mass spectrometer. Elemental analysis was performed on Parkin-Elmer 2400. GC analyses were performed on an FID-GC equipped with a $15\text{ m} \times 3\ \mu\text{m}$ phenyl silicon based capillary column. UV-Vis absorption spectra were recorded on a JASCO V570 spectrophotometer.

Irradiation procedure: 3-Piperidino-1,2-benzisothiazole derivatives were dissolved in MeCN or other solvent used, the resulting solution was allowed into a quartz cuvette and purged by argon, then irradiation was performed by a 1-kW high pressure mercury lamp or 400-W Xe-lamp using appropriate glass filters.

Materials preparation:

2,2'-Dithiobis[5-nitrobenzoic acid]¹⁰: To a dry EtOH (50 mL) solution of 2-chloro-5-nitrobenzoic acid (5.14 g, 25 mmol), potassium *t*-butoxide (2.89 g, 25.0 mmol) was added portion wise to the stirred solution under nitrogen atmosphere at ambient temperature. Resulting mixture was added to dry EtOH (25 mL), and refluxed for 15 min. A solution of sodium sulfide (9.31 g, 12.6 mmol) and sulfur (0.44 g, 13.8 mmol) in water (150 mL) was added slowly to the reaction vessel and resulting solution was refluxed for 10 h. After cooling to room temperature, the reaction mixture was acidified to pH 3–4 with hydrochloric acid. The resulting solids were collected by suction filtrations, washed with water, and dry under vacuum to give 2,2'-dithiobis[5-nitrobenzoic acid], (4.31 g, 10.8 mmol, yield 87.0%) as pale yellow powder.

^1H NMR 400MHz (DMSO- d_6), δ = 8.51 (1H, d, J = 2.7Hz, H4), 8.16 (1H, dd, J = 8.9, 2.7 Hz, H6), 7.67 (1H, d, J = 8.9, H7).

5-Nitro-1,2-benzisothiazole-3(2H)-one¹⁰: A mixture of 2,2'-dithiobis[5-nitrobenzoic acid] (4.04 g, 10.0

mmol), thionyl chloride (4.39 g, 59.3 mmol), and DMF (72 μ L) in CH_2Cl_2 (50 mL) was refluxed. Then, evaporation of solvents gave crude oil. A mixture of the crude oil and bromine (2.0 mL, 38.9 mmol) in $\text{CH}_2\text{ClCH}_2\text{Cl}$ (50 mL) was stirred for 20 min at room temperature and then heated at reflux for 4 h. The residue remaining after evaporation of solvent was dissolved in $\text{CH}_2\text{ClCH}_2\text{Cl}$ (50 mL) at 0 °C in an ice bath, and was added 25 % ammonium hydroxide (25 mL) to the reaction mixture at the same temperature. The solution was stirred at 0 °C for 20 min and at ambient temperature for 16 h. After cooling to 0 °C, the reaction mixture was acidified to pH 3-4 with hydrochloric acid. The resulting solids were collected by suction filtrations, washed with water, and dried under vacuum to give 5-nitro-1,2-benzisothiazole-3(2*H*)-one (3.62 g, 18.4 mmol, yield 92.3%) as pale yellow plates.

^1H NMR 400MHz (DMSO- d_6), δ = 8.60 (1H, d, J = 2.0Hz, H4), 8.40 (1H, dd, J = 8.9, 2.0 Hz, H6), 8.28 (1H, d, J = 8.9, H7).

3-Methoxy-5-nitro-1,2-benzisothiazole¹⁰: 5-Nitro-1,2-benzisothiazole-3(2*H*)-one (1.02 g, 5.1 mmol) was dissolved in dry DMF (15 mL). Potassium carbonate (1.07 g, 7.7 mmol) and then methyl iodide (1.7 mL, 25.9 mmol) was added to the stirred solution of 5-nitro-1,2-benzisothiazole-3(2*H*)-one under nitrogen atmosphere at room temperature and for the reaction mixture was stirred over night. The reaction mixture was poured into ice-water (50 mL), and acidified to pH 3-4 with hydrochloric acid. The aqueous mixture was extracted with three portions of 90 mL EtOAc, combined organic layer was washed with water and brine, dried over Na_2SO_4 , and evaporated to give the crude oil. Purification by chromatography on silica gel eluting with CH_2Cl_2 -hexane (1:1) to give 3-methoxy-5-nitro-1,2-benzisothiazole (421 mg, yield 39.3%) as yellow powder.

^1H NMR 400MHz (CDCl_3), δ = 8.79 (1H, d, J = 2.2Hz, H4), 8.37 (1H, dd, J = 8.9, 2.7 Hz, H6), 7.89 (1H, d, J = 8.9, H7), 4.24 (3H, s, $-\text{OCH}_3$). GC-MS m/z : 210.

3-Chloro-5-nitro-1,2-benzisothiazole¹⁰: A mixture of 3-methoxy-5-nitro-1,2-benzisothiazole (3.53 g, 17.7 mmol), phosphorus oxychloride (14 mL, 148 mmol), and tributylamine (4.3 mL, 17.3 mmol) are stirred at 115 °C for 6 h, and ambient temperature for over night. The reaction mixture was poured into ice-water (50 mL), and the aqueous mixture was extracted with three portions of 90 mL CH_2Cl_2 . Combined organic layer was washed with water and saturated aqueous NaHCO_3 , dried over anhydrous Na_2SO_4 , and evaporated, to give crude oil. Purification by chromatography on silica gel eluting with CH_2Cl_2 to give 3-chloro-5-nitro-1,2-benzisothiazole, (3.10 g, yield 81.8%) as orange color plates.

^1H NMR 400MHz (CDCl_3), δ = 8.93 (1H, d, J = 2.0Hz, H4), 8.47 (1H, dd, J = 8.9, 2.0 Hz, H6), 8.08 (1H, dd, J = 8.9, 0.5 Hz, H7).

3-Chloro-1,2-benzisothiazole: 3-Chloro-1,2-benzisothiazole was prepared by a similar method with 3-chloro-5-nitro-1,2-benzisothiazole. Purification by distillation of brown oil (bp 95–98 °C /9 mmHg),

gave the product (6.97 g, yield 46.4%) as colorless solid.

^1H NMR 400MHz (CDCl_3), δ = 8.04 (1H, ddd, J = 8.1, 1.0, 1.0 Hz, H4), 7.92 (1H, ddd, J = 8.3, 1.0, 1.0 Hz, H7), 7.61 (1H, ddd, J = 8.3, 7.1, 1.0 Hz, H6), 7.53 (1H, ddd, J = 8.1, 7.1, 1.0 Hz, H5).

3-Chloro-7-nitro-1,2-benzisothiazole: A mixture of 3-chloro-1,2-benzisothiazole (2.26 g, 13.3 mmol) dissolved in 96% sulfuric acid (8 mL) was cooled over ice-water bath. Finely powdered potassium nitrate (1.23 g, 12.2 mmol) dissolved in 96% sulfuric acid (4 mL) was slowly added portion wise to the stirred solution of 3-chloro-1,2-benzisothiazole at 0 °C and kept at 0 °C with stirring for 3 h. Resulting mixture was poured into ice cold water (150 mL). The resulting solids were collected by suction filtration, washed with water, and dried under vacuum. Purification by chromatography on silica gel eluting with CHCl_3 –hexane (7:3) to give 3-chloro-7-nitro-1,2-benzisothiazole (429 mg, yield 15.0%) as pale yellow powder.

^1H NMR 400MHz (CDCl_3), δ = 8.59 (1H, dd, J = 7.9 Hz, H6), 8.40 (1H, dd, J = 5.8 Hz, H4), 7.77 (1H, dd, J = 7.9 Hz, H5). GC-MS m/z 263.

5-Nitro-3-piperidino-1,2-benzisothiazole (1a)⁹: A mixture of piperidine (6.00 mL, 101 mmol) and 3-chloro-5-nitro-1,2-benzisothiazole (310 mg, 1.40 mmol) was refluxed with stirring for overnight, and excess piperidine was evaporated off, to give a crude oil. The mixture was partitioned between CH_2Cl_2 (30 mL) and water (30 mL), the aqueous layer was extracted with CH_2Cl_2 (2 × 30 mL), and the combined organic layers were washed with water (20 mL), dried over anhydrous Na_2SO_4 , and evaporated, to give the crude oil. Purification by chromatography on silica gel eluting with CHCl_3 , and crystallization from CH_2Cl_2 –hexane to give **1a** (121 mg, yield 32.8%) as orange color plates.

^1H NMR 400MHz (CDCl_3), δ = 8.79 (1H, d, J = 2.4 Hz, H4), 8.30 (1H, dd, J = 9.0, 2.0 Hz, H6), 7.89 (1H, d, J = 9.0 Hz, H7), 3.53 (4H, t, J = 5.4 Hz, $-\text{NCH}_2-$), 1.86-1.84 (4H, m, $-\text{CH}_2-$), 1.72-1.65 (2H, m, $-\text{CH}_2-$). GC-MS m/z : 263. Anal. Calcd for $\text{C}_{12}\text{H}_{13}\text{N}_3\text{O}_2\text{S}$: C, 54.74; H, 4.98; N, 15.96. Found: C, 54.56; H, 4.83; N, 16.03.

3-Piperidino-1,2-benzisothiazole (1c)⁹: **1c** was prepared according to a similar method to prepare **1a**. Purification by chromatography on silica gel eluting with hexane–EtOAc (9:1) to give **1c** (456 mg, yield 70.8%) as colorless oil.

^1H NMR 400MHz (CDCl_3), δ = 7.91 (1H, dd, J = 8.0, 1.0 Hz, H4), 7.80 (1H, dd, J = 8.3, 1.0 Hz, H7), 7.46 (1H, td, J = 8.3, 1.0 Hz, H6), 7.35 (1H, td, J = 8.0, 1.0 Hz, H5), 3.49-3.46 (4H, t, J = 5.5 Hz, $-\text{NCH}_2-$), 1.83-1.76 (4H, m, $-\text{CH}_2-$), 1.72-1.65 (2H, m, $-\text{CH}_2-$). GC-MS m/z : 218. Anal. Calcd for $\text{C}_{12}\text{H}_{14}\text{N}_2\text{S}$: C, 66.02; H, 6.46; N, 12.83. Found: C, 66.33; H, 6.21; N, 13.08.

7-Nitro-3-piperidino-1,2-benzisothiazole (1b)⁹: **1b** was prepared by a similar method to prepare **1a**. Purification by silica gel chromatography eluting with CHCl_3 and by crystallization from EtOH gave **1b**

(58.5 mg, yield 49.4%) as red crystals.

^1H NMR 400MHz (CDCl_3), δ = 8.46 (1H, dd, J = 7.1Hz, H6), 8.25 (1H, dd, J = 7.1Hz, H4), 7.56 (1H, t, J = 7.9, H5), 3.49 (4H, t, J = 5.7 Hz, $-\text{NCH}_2-$), 1.67-1.84 (6H, m, $-\text{CH}_2-$). GC-MS m/z : 263. Anal. Calcd for $\text{C}_{12}\text{H}_{13}\text{N}_3\text{O}_2\text{S}$: C, 54.74; H, 4.98; N, 15.96. Found: C, 54.64; H, 4.88; N, 15.98.

5-Nitro-3-piperidino-1,3-benzthiazole (2a)⁹: A mixture of piperidine (4.0 mL, 68 mmol) and 2-chloro-5-nitro-1,3-benzothiazole (420 mg, 1.90 mmol) was refluxed with stir for 2 h, and excess piperidine was evaporated to give crude oil. The mixture was partitioned between CH_2Cl_2 (30 mL) and water (30 mL), the aqueous layer was extracted with CH_2Cl_2 (30 mL), and the combined organic layers were washed with water (20mL), dried over anhydrous Na_2SO_4 , and evaporated, to give the crude yellow solid. Purification by chromatography on silica gel eluting with CHCl_3 to give **2a** (408 mg, yield 81.5%) as yellow plates.

^1H NMR 400MHz (CDCl_3), δ = 8.31 (1H, d, J = 2.2 Hz, H4), 7.91 (1H, dd, J = 8.6, 2.2 Hz, H6), 7.65 (1H, d, J = 8.6 Hz, H7), 3.65 (4H, m, $-\text{NCH}_2-$), 1.73 (6H, m, $-\text{CH}_2-$). GC-MS m/z : 263. Anal. Calcd for $\text{C}_{12}\text{H}_{13}\text{N}_3\text{O}_2\text{S}$: C, 54.74; H, 4.98; N, 15.96. Found: C, 54.66; H, 4.88; N, 15.75.

3-Piperidino-1,3-benzthiazole (2c)⁹: A mixture of piperidine (1.06 g, 21.5 mmol) and sodium bicarbonate (2.10 g, 25.0 mmol) in 2-propanol (88 mL) was refluxed with stirring for 1 h. A solution of 2-chloro-1,3-benzothiazole (1.06 g, 6.25 mmol) in 2-propanol (5.0 mL) was added slowly into the stirred solution at ambient temperature. The mixture was refluxed for 24 h. The excess piperidine was removed by evaporation, to give a crude oil. The mixture was partitioned between CH_2Cl_2 (30 mL) and water (30 mL), the aqueous layer was extracted with CH_2Cl_2 (30 mL), and the combined organic layers were washed with water (20 mL), dried over anhydrous Na_2SO_4 , and evaporated, to give the crude yellow solid. Purification by crystallization from CH_2Cl_2 / hexane gave **2c** (866 mg, yield 63.5%) as pale yellow plates.

^1H NMR 400MHz (CDCl_3), δ = 7.58 (1H, dd, J = 8.0, 1.0 Hz, H4), 7.53 (1H, dd, J = 8.0, 1.0 Hz, H7), 7.27 (1H, ddd, J = 8.0, 8.0, 1.0 Hz, H6), 7.04 (1H, ddd, J = 8.0, 8.0, 1.0 Hz, H5), 3.61-3.59 (4H, m, $-\text{NCH}_2-$), 1.71-1.69 (6H, m, $-\text{CH}_2-$). GC-MS m/z : 218. Anal. Calcd for $\text{C}_{12}\text{H}_{14}\text{N}_2\text{S}$: C, 66.02; H, 6.46; N, 12.83. Found: C, 65.98; H, 6.28; N, 12.94.

7-Nitro-3-piperidino-1,3-benzthiazole (2b): A solution of **1b** in MeCN (3 mL, 3.9×10^{-4} M) under argon was exposed to a low pressure mercury lamp (254 nm) for 24 h, giving the product with quantitative yield. Purification by crystallization from CHCl_3 , gave **2b** (yield 46%) as colorless powder.

^1H NMR 400MHz (CDCl_3), δ = 8.02 (1H, dd, J = 11.0, 1.1 Hz, H4), 7.78 (1H, dd, J = 11.0, 1.1 Hz, H6), 7.41 (1H, dd, J = 11.0, 11.0 Hz, H5), 3.93-3.65 (4H, m, $-\text{NCH}_2-$), 1.76-1.68 (6H, m, $-\text{CH}_2-$). GC-MS m/z : 263.

Computational method: Quantum chemical calculations were performed for all examined

2-piperidino-1,2-benzisothiazoles, 1,3-benzothiazoles, and intermediates. Molecular geometries were fully optimized by using density functional theory (DFT) with standard B3LYP functional and 6-31G* basis set, applying the Spartan-'06 Win.¹¹ All the calculations were performed for the compounds with absolute configuration. The ground states geometries optimized in this manner gave relative energies of the compounds. Excited-state energies, oscillator strengths of the transitions, and molecular orbitals including frontier orbitals (HOMO-LUMO) were obtained by using time-dependent DFT (TD-DFT) method by Gaussian'03 Rev. B.0.3 suite¹² of programs using 6-31++G(d) basis set.

ACKNOWLEDGEMENTS

The authors thank Analytical Center of Chiba University for her assistance of characterization of the compounds. This research project was financially supported by Grants-in-Aid for Scientific Research (No. 20550056) from the Ministry of Education, Culture, Sports, Science, and Technology (MEXT).

REFERENCES

1. T. F. Seeger, P. A. Seymour, A. W. Schmidt, S. H. Zorn, D. W. Shulz, L. A. Lebel, S. McLean, V. Guanowsky, H. R. Howard, J. A. III, Lowe, and J. Heym, *J. Pharmacol. Expt. Therapeutics*, 1995, **275**, 101.
2. H. R. Howard, J. A. III, Lowe, T. F. Seeger, P. A. Seymour, S. H. Zorn, P. R. Maloney, F. E. Ewing, M. E. Newman, A. W. Schmidt, J. S. Furman, G. L. Robinson, E. Jackson, C. Johnson, and J. Morrone, *J. Med. Chem.*, 1996, **39**, 143.
3. Y. Miyake, J. Sakai, M. Shibata, N. Yonekura, I. Miura, K. Kumakura, and K. Nagayama, *J. Pestic. Sci.*, 2005, **30**, 390.
4. J. W. Pavlik and E. M. Kurzweil, *J. Org. Chem.*, 1991, **56**, 6316.
5. a) J. W. Pavlik and P. Tongcharoensirikul, *J. Org. Chem.*, 2000, **65**, 3626; b) J. W. Pavlik, P. Tongcharoensirikul, N. P. Bird, A. C. Day, and J. A. Barltrop, *J. Am. Chem. Soc.*, 1994, **116**, 2292; c) A. Sipos and S. Berenyl, *Monatsh. Chem.*, 2009, **140**, 387.
6. J. W. Pavlik, 'CRC HANDBOOK OF Organic Chemistry and Photochemistry and Photobiology,' 2ed., ed. by W. Horspool and F. Lenci, CRC Press LLC, Boca Raton, 2004, ss. 98.
7. M. D'Auria, *Tetrahedron*, 2002, **58**, 8037.
8. T. R. Sharp, K. R. Leeman, D. E. Bryantb, and G. J. Horana, *Tetrahedron Lett.*, 2003, **44**, 1559.
9. H. Tanikawa, K. Ishii, S. Kubota, S. Yagai, A. Kitamura, and T. Karatsu, *Tetrahedron Lett.*, 2008, **49**, 3444.
10. L. Zhu, M. Zhang, and M. Dai, *J. Heterocycl. Chem.*, 2005, **42**, 727.
11. a) Spartan'06, Wavefunction, Inc. Irvine, CA; b) J. Kong, C.A. White, A.I. Krylov, C.D. Sherrill, R.D.

- Adamson, T.R. Furlani, M.S. Lee, A.M. Lee, S.R. Gwaltney, T.R. Adams, C. Ochsenfeld, A.T.B. Gilbert, G.S. Kedziora, V.A. Rassolov, D.R. Maurice, N. Nair, Y. Shao, N.A. Besley, P.E. Maslen, J.P. Dombroski, H. Daschel, W. Zhang, P.P. Korambath, J. Baker, E.F.C. Byrd, T. Van Voorhis, M. Oumi, S. Hirata, C.-P. Hsu, N. Ishikawa, J. Florian, A. Warshel, B.G. Johnson, P.M.W. Gill, M. Head-Gordon, and J.A. Pople, *J. Computational Chem.*, 2000, **21**, 1532.
12. M. J. Frisch, G. W. Trucks, H. B. Schlegel, G. E. Scuseria, M. A. Robb, J. R. Cheeseman, J. A. Montgomery Jr., T. Vreven, K. N. Kudin, J. C. Burant, J. M. Millam, S. S. Iyengar, J. Tomasi, V. Barone, B. Mennucci, M. Cossi, G. Scalmani, N. Rega, G. A. Petersson, H. Nakatsuji, M. Hada, M. Ehara, K. Toyota, R. Fukuda, J. Hasegawa, M. Ishida, T. Nakajima, Y. Honda, O. Kitao, H. Nakai, M. Klene, X. Li, J. E. Knox, H. P. Hratchian, J. B. Cross, C. Adamo, J. Jaramillo, R. Gomperts, R. E. Stratmann, O. Yazyev, A. J. Austin, R. Cammi, C. Pomelli, J. W. Ochterski, P. Y. Ayala, K. Morokuma, G. A. Voth, P. Salvador, J. J. Dannenberg, V. G. Zakrzewski, S. Dapprich, A. D. Daniels, M. C. Strain, O. Farkas, D. K. Malick, A. D. Rabuck, K. Raghavachari, J. B. Foresman, J. V. Ortiz, Q. Cui, A. G. Baboul, S. Clifford, J. Cioslowski, B. B. Stefanov, G. Liu, A. Liashenko, P. Piskorz, I. Komaromi, R. L. Martin, D. J. Fox, T. Keith, M. A. Al-Laham, C. Y. Peng, A. Nanayakkara, M. Challacombe, P. M. W. Gill, B. Johnson, W. Chen, M. W. Wong, C. Gonzalez, J. A. Pople, Gaussian 03, Revision B.03, Gaussian, Inc., Pittsburgh, PA, 2003.